creative commons

C O M M O N S D E E D

저작자표시-비영리-변경금지 2.0 대한민국

이용자는 아래의 조건을 따르는 경우에 한하여 자유롭게

- 이 저작물을 복제, 배포, 전송, 전시, 공연 및 방송할 수 있습니다.

다음과 같은 조건을 따라야 합니다:

저작자표시. 귀하는 원저작자를 표시하여야 합니다.

비영리. 귀하는 이 저작물을 영리 목적으로 이용할 수 없습니다.

변경금지. 귀하는 이 저작물을 개작, 변형 또는 가공할 수 없습니다.

- 귀하는, 이 저작물의 재이용이나 배포의 경우, 이 저작물에 적용된 이용허락조건을 명확하게 나타내어야 합니다.
- 저작권자로부터 별도의 허가를 받으면 이러한 조건들은 적용되지 않습니다.

저작권법에 따른 이용자의 권리는 위의 내용에 의하여 영향을 받지 않습니다.

이것은 이용허락규약(Legal Code)을 이해하기 쉽게 요약한 것입니다.

Disclaimer

dCollection

의학석사 학위논문

Computer-Assisted Detection of Retinal Nerve Fiber Layer Defect on Fundus Photography with the Average Curvature of Polarimetric Image

극갈림 영상의 평균곡률을 이용한 안저사진상 망막신경섬유층 결손의 컴퓨터-보조 검출

2015 년 2 월

서울대학교 대학원

의학과 안과학전공

이 진 호

Computer-Assisted Detection of Retinal Nerve Fiber Layer Defect on Fundus Photography with the Average Curvature of Polarimetric Image

지도 교수 박 기 호

이 논문을 의학석사 학위논문으로 제출함
2014 년 10 월

서울대학교 대학원
의학과 안과학과정
이 진 호

이진호의 의학석사 학위논문을 인준함
2014 년 12 월

위 원 장 김 희 찬 (인)

부위원장 김 성 준 (인)

위 원 박 기 호 (인)

Abstract

Purpose

To develop novel software to determine whether there is a retinal nerve fiber layer (RNFL) defect in a given fundus image and, if there is, where it presents.

Methods

The given fundus photography was rotated to non-extorted image. The intensity profile was normalized to enhance the contrast, and then the region of interest (ROI) was set as the circumferential area surrounding the optic disc (internal diameter: 2 disc diameters [DD], external diameter: 3 DD). The temporal half of ROI was converted to a polarimetric image. After removing the blood vessels using Frangi filter, the differential gradients and the average curvatures were calculated sector-by-sector and the local maximum values were obtained. If the local maximum curvature was greater than the cut-off value, the sector was considered to be an RNFL defect.

The images of 100 normal healthy controls and 100 open-angle glaucoma patients were enrolled as age- and sex-matched samples. When both of a subject s eyes were eligible, the image of one eye was randomly selected. Maximum curvatures were compared and a receiver operating characteristic (ROC) analysis was performed to determine the validity of the algorithm and to set up the optimum cut-off value.

Results

There were no significant differences in age or gender (p=0.456, p=0.396, respectively) between the two groups. In the glaucoma group, the mean deviation was -4.90 ± 5.40 dB. There was, however, a significant difference of maximum curvature (14.37 ± 5.13 in control group, 20.67 ± 10.56 in glaucoma group, p<0.001). The area under ROC curve was 0.711 (95% CI; 0.639 - 0.782). The positive likelihood ratio was maximized to 1.84 with a sensitivity of 70.0% and a specificity of 62.0%. When a specificity was set to 50.0% which was minimum acceptable value, the positive likelihood ratio was determined to 1.50 with a sensitivity of 74.8%.

Conclusions

The proposed software can be an effective tool for automated detection of RNFL defect.

Keywords: Computer-aided diagnosis, Fundus photography, Retinal nerve fiber layer, Glaucoma

Student number: 2013-21692

CONTENTS

LIST OF FIGURES

Introduction

Glaucoma is one of the leading causes of irreversible blindness worldwide. About 60.5 million people suffer from primary open-angle glaucoma (POAG) and primary angle-closure glaucoma (PACG),(1) which number is expected to increase to 111.8 million by 2040.(2) However, due to glaucoma's slow progression, many patients do not present any symptoms before the disease has become advanced. Therefore, an early-detection tool for asymptomatic-stage glaucoma is essential.(3)

An important component of glaucoma diagnostics is retinal nerve fiber layer (RNFL) evaluation. It is known that RNFL changes appear earlier than either visual field (VF) defects or optic nerve head (ONH) changes.(4-6) Fundus photography is the tool of choice of primary physicians and health-screening programs where specialized techniques such as optical coherence tomography (OCT) or scanning laser polarimetry are unavailable. Automated detection of RNFL defect on fundus photography, moreover, can be a very effective glaucoma-screening modality. Thus, for general ophthalmologists or primary eye-care physicians, an automated algorithm for objective RNFL evaluation based on fundus photography instead of expensive instruments such as OCT can be an economical as well as effective means of early-glaucoma detection.

Studies on fundus-photography-based RNFL analysis are available in the literature. Kim et al. derived a computer densitometry of the RNFL from first derivatives.(7, 8) Muramatsu et al. reported acceptable results for the utilization of the Gabor filter in detecting the edges of RNFL defect areas.(9, 10) Bock et al. derived a glaucoma prediction model based on color disc photography,(11) but they did not analyze RNFL defects. Notwithstanding all of these important advances, to our knowledge there is as yet no algorithm developed that utilizes second derivatives and average curvatures for the purposes of RNFL defect screening.

We developed novel software that determines, on the basis of average curvature, whether there is an RNFL defect in a given fundus image and, if there is, where it presents. Our aim in the present study was to evaluate the diagnostic validity of the proposed software.

Methods

Preprocessing

Image normalization and enhancement

RNFL visibility is maximized on red-free images rather than color photography.(12) Accordingly, a color fundus image was converted to a red-free image using green channel, whereby the image was mirrored in the case of the left eye. In the next step, the image was rotated to position the center of the ONH at the same level as the macula and facilitate further analysis thereby. Finally, the image was resized so that the distance between the centers of the ONH and macula was 400 pixels.

Determination of fundus region

The elimination of the background region is an essential step in medical image processing, specifically to reduce computational complexity and apply the algorithm effectively to the regions of interest (ROIs), namely, in the present case, the fundus region. In the given fundus image I(x,y), in which (x,y) is a pixel location, it is relatively straightforward to obtain the set of pixels in the ROI Ω_{eye} by applying the following hard thresholding:

$$\Omega_{eye} = \{(x,y) | I(x,y) > T_{eye}\}. \quad (1)$$

In (1), T_{eye} is a fixed threshold, which was set to 10 in this study for optimal contrast.

Background brightness correction

Due to the sensitivity of the fundus camera, which is mainly used for fundus imaging, background brightness correction plays a crucial role in glaucoma screening, specifically in vessel elimination, macular region detection, and optic disc region determination. Brightness correction is equivalent to intensity normalization of varied images taken in different environments and according to different axial lengths of eyeball. To normalize variations, we defined the mapping function as

$$f_{normal} : [0,1] \times \Omega_{eye} \rightarrow [\mu - 1.96\sigma, \quad \mu + 1.96\sigma] \times \Omega_{eye} \quad (2)$$

where μ and σ are the mean and standard deviation of pixel intensities inside of Ω_{eye}.

Setting of region of interest (ROI)

The ROI here indicates the circumferential area surrounding the ONH. To set the ROI, the optic disc and the macula were determined in a fully automated manner. This determination, in generating the major and minor axes of fundus images, plays a critical role in localizing the sectors; localization of the optic disc's center of mass, furthermore, is an essential step for calculation of average curvature. To that end, we exploited the prior knowledge of the location and intensity of the ROIs, where the optic discs undoubtedly show the highest intensity, while the macular regions are formed within a certain distance and direction relative to the optic discs, with lower intensity in fundus images. Accordingly, we obtained the probability density function (PDF) of the optic disc by means of the Gaussian mixture model (GMM), the peak of which represented the highest intensity value in the histogram. Then, the pixels were set to the region of the optic disc, the intensity values of which were within the 99% confidence interval (CI) of the PDF from which the center of mass (utilized as a reference point for the determination of the macular region) was computed. By thorough investigation, the candidate macular location was found. Then, the PDF having the lowest intensity values was chosen as the macular region. Finally, the circumferential area surrounding the ONH was defined (internal diameter: 2 disc diameters [DD], external diameter: 3 DD) (Figure 1).

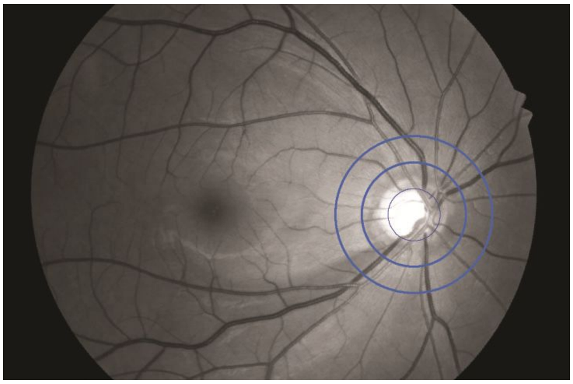

Figure 1. Example of ROI conversion to polarimetric image.

The normalized fundus image is shown, and the ROI is drawn between the two blue circles.

RNFL defect detection method

Image polarization

The temporal half of the ROI was converted to a polarimetric image by normalizing the intensity profile using the mode value, resizing the segment of the ROI (from trapezoid to rectangular shape) (Figure 3a) in which blood vessels were detected with vessel masks using a Frangi filter (Figure 2),(13) and removing the blood vessels from the polarized image (Figure 3b).

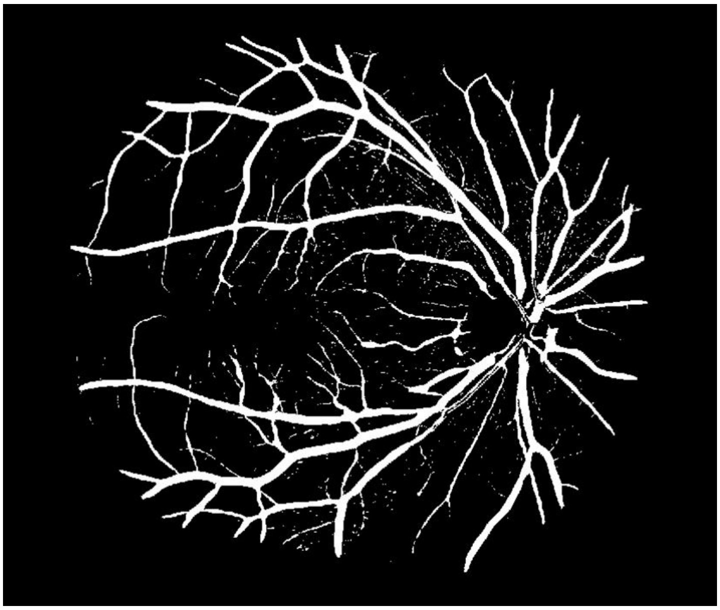

Figure 2. Detection of retinal blood vessels with vessel masks using Frangi filter

Calculation of differential gradients and average curvatures

The differential gradients of the polarized image were calculated along the angular axis of the defined ROI, after which a noise-canceling procedure was carried out. After the calculation of the gradient data using first derivatives of intensity plot, the average curvature was calculated sector-by-sector with the second derivatives along the angular axis. The residual significant noises has decreased sharply with average curvature. From the plot of the average curvature, the maximum value was obtained (Figure 3c). Finally, the sector greater than the pre-defined cut-off value was determined to be the RNFL defect (Figure 4).

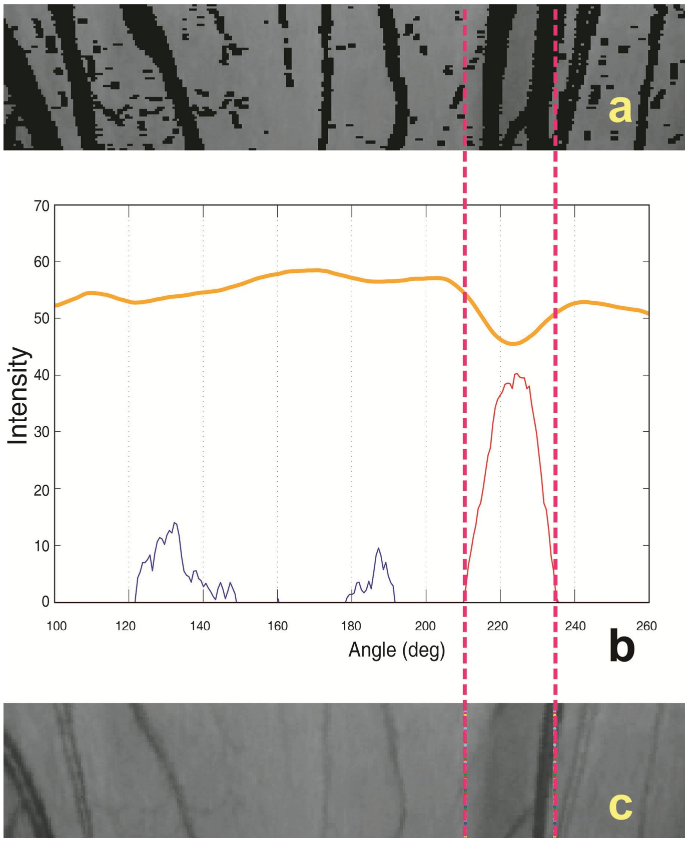

Figure 3. Polarimetric technique and process of RNFL defect detection.

The corresponding angular axes are marked with vertical dashed lines in the images.

a. Original polar images before removal of blood vessels

b. Differential gradients calculated along angular axis (upper solid line) and their mean curvature (cyan: false defect to be ignored, magenta: true RNFL defect)

c. New polar image indicating true RNFL defect region

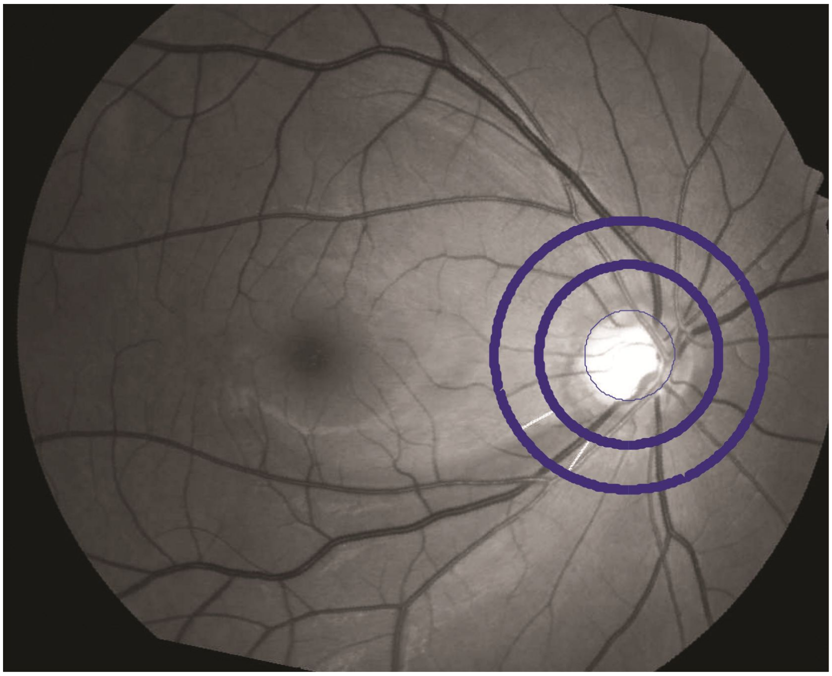

Figure 4. Final output of program.

The RNFL defect is presented as white solid lines in the original red-free fundus image.

Participants

The subjects in the study were selected from Seoul National University Hospital (Korea)'s glaucoma clinic database from 2009 to 2012. One hundred early-stage open-angle glaucoma patients and 100 age- and sex-matched healthy controls were enrolled. Those with retinal diseases severely affecting the RNFL (e.g. severe epiretinal membrane, proliferative diabetic retinopathy or pathologic high myopia) were excluded. Glaucomatous eyes were defined as having a glaucomatous VF defect confirmed by two reliable Humphrey

Field Analyzer (C30-2 SITA Standard, Carl Zeiss Meditec, Dublin, CA)-based VF examinations and by the presence of glaucomatous optic disc cupping irrespective of the level of IOP. Glaucomatous optic disc cupping was defined as neuroretinal rim thinning, notching, excavation, or RNFL defect with corresponding VF deficit. The control subjects had an intraocular pressure (IOP) of ≤ 21 mmHg with no history of increased IOP, absence of glaucomatous disc appearance, a normal VF defined by a normal Glaucoma Hemifield Test, as well as a mean deviation and pattern standard deviation within the normal limits.(14,15) One eye was randomly selected if both eyes were eligible. Fundus photographs were taken using a Canon digital fundus camera (CF-60UVi; Canon, Utsunomiya, Japan).

The research followed the tenets of the Declaration of Helsinki, and the protocol was approved by the local ethical committee.

Statistical analysis

Comparisons of maximum curvatures between the glaucoma and control groups were made with the independent *t*-test. The diagnostic performance of the new test was determined by receiver operating characteristic (ROC) analysis. The sensitivity and specificity values were computed for all of the possible cut-off values of the maximum curvatures. Also, the positive likelihood ratios (LRs) were computed using the formula

$$LR = \frac{sensitivity}{1 - specificity}.$$

To find the optimal cut-off value, the ROC-curve point maximizing the LR was determined, and the Youden index (sensitivity + specificity - 1) was calculated.

Results

The study, as noted above, included 100 patients with open-angle glaucoma and 100 healthy controls. The mean ages of the control and glaucoma groups were 57.5 ± 12.8 and 58.7 ± 11.2 years, respectively (p=0.456). In the control group, 52 of the 100 subjects were male, while in the glaucoma group, 45 were male (p=0.396, Fischer's exact test). The mean deviations of VF, obtained on the same day as the imaging, were -4.90 ± 5.40 and +0.45 ± 1.52 dB, respectively. The circumpapillary RNFL thicknesses on OCT were 83.2 ± 6.57 and 96.1 ± 4.25 μm, respectively. The difference of maximum curvature (14.37 ± 5.13 in control group, 20.67 ± 10.56 in glaucoma group, p<0.001) was statistically significant.

In the ROC analyses, the maximum curvature was highly associated with RNFL defect. The area under curve (AUC) was 0.711 (95% CI; 0.639 - 0.782). The probability of asymptomatic significance was less than 0.001. In the sensitivity range of 65.0 to 90.0%, the LR was maximized to 1.84 with a sensitivity of 70.0% and a specificity of 62.0%, for a cut-off value of 14.84. The Youden index was then calculated to 0.32. When a specificity was set minimum acceptable value of 50.0%, the LR was determined to 1.50 with a sensitivity of 74.8%.

Discussion

The purpose of this new software was to assist physicians' fundus-image-based diagnosis of glaucoma. For patients visiting glaucoma clinics, many specialized imaging instruments and VF tests are available, whereas for patients seeking treatment by primary eye-care physicians or in underdeveloped regions generally, typically only fundus photography is offered.

The central data of this study, namely the AUC of 0.711, is encouraging. The first objective of the RNFL defect screening program is to provide physicians with additional information on possible RNFL defect areas, not to obviate their judgment. It should be noted that the effectiveness of the software might have been underestimated, due to the fact that the selected glaucoma patients were all at the early stage, which made the difference of maximum average curvature, used to judge RNFL defect between the two groups, smaller. If the glaucoma group had been selected more evenly to include, as in a real clinical situation, all progression stages, the ROC analysis result would have been even better.

For determination of optimum cut-off value, we considered the positive likelihood ratio (LR) which corresponds well to the purpose of assisting primary physicians' decision. On the other hand, as this software is targeted at screening test rather than confirmation, it may be preferable to reduce specificity (meaning a lower cut-off) in order to increase the sensitivity. However, setting the specificity to 50.0%–which is minimum acceptable value–, the sensitivity has increased to just 74.8%. Considering the result of ROC analysis, choosing the cut-off value for maximizing the positive LR may be justified.

There have been similar previous studies involving RNFL defect detection along a circular (or hyperbolic) ROI. Kim et al.(7) developed a program for quantitative measurement of RNFL atrophy, though it was not fully automated; accordingly, the optic disc margin and macula had to be localized manually. Fully automated ONH, fovea, and retinal blood vessel localization techniques eventually were developed,(14) some years after which Lee et al.(8) reported an automatic RNFL defect quantification method. Similarly to our study, they drew an intensity plot to detect sudden intensity change; however, they had no compensation algorithm for retinal vessels, using only first derivatives. Hayashi et al.(9, 10) used the Gabor filter to enhance RNFL defect contrast, and introduced a linear discriminant analysis (15) and an artificial neural network(16) as classifiers. These two classifiers are excellent models that have a long tradition in computer science; but because of the limited number of cases, they used leave-one-out test methods. Also, the center of the ONH was determined manually, the algorithm assuming it to be located horizontally to the macula, which approach can incur significant error with polarimetric techniques. The result has been poorer, furthermore, in cases of diffuse RNFL defect. Bock et al.(11) proposed a data-driven framework based on colored optic disc photographs. The calculated glaucoma risk index showed good glaucoma detection results. However, Chauhan et al.(17, 18) recently showed that the clinically visible disc margin cannot reflect the true outer border of the rim tissue, and that disc-margin-based rim tissue assessment, therefore, might be significantly erroneous.

The key remedial step, attempted here for the first time, is the computation of the second derivatives and average curvatures along the angular axis of a polar image. In the present study, after calculating the first derivatives of the intensity plot of a polar image, there were unignorable noises potentially leading to false positives, despite the application of a smoothing filter. Calculating the "average" curvatures in the angular sectors from the second derivatives, however, significantly reduced the noises.

Despite the additional noise-canceling procedure, there were some cases of false classification. The main reasons were poor dilation, severe media opacity, diffuse retinal atrophy, and very-early-stage slit-like RNFL defects. Algorithm also has theoretical weak points. At first, it divides the ROI by angular axis equally, however, the actual RNFL runs hyperbolically. Moreover, the algorithm is unable to detect a defect outside the ROI. Further study will be needed for analysis of hyperbolic RNFL defect and automatic detection of the optic disc rim. Upon optic disc rim detection, the probable RNFL defect area would be determined more accurately in relation to the corresponding region of rim thinning.

In conclusion, the proposed novel software can be an economical as well as an effective tool for early detection of glaucomatous RNFL defect.

References

1. Kingman S. Glaucoma is second leading cause of blindness globally. Bulletin of the World Health Organization. 2004;82(11):887-8.
2. Tham YC, Li X, Wong TY, Quigley HA, Aung T, Cheng CY. Global Prevalence of Glaucoma and Projections of Glaucoma Burden through 2040: A Systematic Review and Meta-Analysis. Ophthalmology. 2014.
3. Michelson G, Warntges S, Hornegger J, Lausen B. The papilla as screening parameter for early diagnosis of glaucoma. Deutsches Arzteblatt international. 2008;105(34-35):583-9.
4. Sommer A, Katz J, Quigley HA, et al. CLinically detectable nerve fiber atrophy precedes the onset of glaucomatous field loss. Archives of Ophthalmology. 1991;109(1):77-83.
5. Sommer A, Miller NR, Pollack I, Maumenee AE, George T. The nerve fiber layer in the diagnosis of glaucoma. Archives of ophthalmology. 1977;95(12):2149-56.
6. Medeiros FA, Zangwill LM, Bowd C, Mansouri K, Weinreb RN. The structure and function relationship in glaucoma: implications for detection of progression and measurement of rates of change. Investigative ophthalmology & visual science. 2012;53(11):6939-46.
7. Kim DM, Yi K, Kang KB. Computer Densitometry of Retinal Nerve Fiber layer Photographs. Journal of the Korean Ophthalmological Society. 1998;39(4):708-14.

8. Lee S, Kim K, Seo J, Kim D, Chung H, Park K, et al., editors. Automated quantification of retinal nerve fiber layer atrophy in fundus photograph. Engineering in Medicine and Biology Society, 2004 IEMBS'04 26th Annual International Conference of the IEEE; 2004: IEEE.

9. Hayashi Y, Nakagawa T, Hatanaka Y, Aoyama A, Kakogawa M, Hara T, et al., editors. Detection of retinal nerve fiber layer defects in retinal fundus images using Gabor filtering. Medical Imaging; 2007: International Society for Optics and Photonics.

10. Muramatsu C, Hayashi Y, Sawada A, Hatanaka Y, Hara T, Yamamoto T, et al. Detection of retinal nerve fiber layer defects on retinal fundus images for early diagnosis of glaucoma. Journal of biomedical optics. 2010;15(1):016021.

11. Bock R, Meier J, Nyúl LG, Hornegger J, Michelson G. Glaucoma risk index: Automated glaucoma detection from color fundus images. Medical image analysis. 2010;14(3):471-81.

12. Frisen L. Photography of the retinal nerve fibre layer: an optimised procedure. The British journal of ophthalmology. 1980;64(9):641-50.

13. Frangi AF, Niessen WJ, Vincken KL, Viergever MA. Multiscale vessel enhancement filtering. Medical Image Computing and Computer-Assisted Interventation—MICCAI'98: Springer; 1998. p. 130-7.

14. Sinthanayothin C, Boyce JF, Cook HL, Williamson TH.

Automated localisation of the optic disc, fovea, and retinal blood vessels from digital colour fundus images. British Journal of Ophthalmology. 1999;83(8):902-10.

15. Fisher RA. The use of multiple measurements in taxonomic problems. Annals of eugenics. 1936;7(2):179-88.

16. Rumelhart DE, Hinton GE, Williams RJ. Learning internal representations by error propagation. DTIC Document, 1985.

17. Chauhan BC, O'Leary N, Almobarak FA, Reis AS, Yang H, Sharpe GP, et al. Enhanced detection of open-angle glaucoma with an anatomically accurate optical coherence tomography-derived neuroretinal rim parameter. Ophthalmology. 2013;120(3):535-43.

18. Reis AS, O'Leary N, Yang H, Sharpe GP, Nicolela MT, Burgoyne CF, et al. Influence of clinically invisible, but optical coherence tomography detected, optic disc margin anatomy on neuroretinal rim evaluation. Investigative ophthalmology & visual science. 2012;53(4):1852-60.

국문초록

목적

주어진 안저영상에 망막신경섬유층의 결손이 존재하는지, 존재한다면 어디에 위치하는지 찾아내는 새로운 소프트웨어를 제안하고자 한다.

방법

주어진 안저영상를 회전시키고 대비 증강을 위해 정규화를 실시하였다. 이미지 관심영역을(ROI) 시신경판을 둘러싼 환형의 영역으로 설정하였고(내부직경: 시신경 직경의 2배, 외부직경: 시신경 직경의 3배), 이 중 이측 절반을 극갈림 영상으로 변환하였다. Frangi 필터를 사용하여 극갈림 영상에서 혈관을 제거한 후, 신호밝기의 미분값 및 평균곡률을 일정 구간마다 계산하였고 각 국소 영역마다 그 최대값을 획득하였다. 각 국소영역의 최대 평균곡률이 역치값보다 클 경우 망막신경섬유층 결손으로 결정되었다.

개방각녹내장 환자 100명과 연령 및 성별을 짝짓기한 정상 대조군 100명이 포함되었다. 양안 모두 연구에 적합한 경우 임의로 한 눈만 선택하였다. 양 군간의 최대 곡률을 비교하였고, 수신자 동작 특성 분석을 시행하여 알고리즘의 정확성을 검증하고 적절한 절단값을 결정하였다.

결과

양 군 간에 나이와(p=0.456) 성별은(p=0.396) 유의한 차이가 없었다. 녹내장 군에서 험프리시야계상 평균편위는(mean deviation) −4.90 ± 5.40 dB 이었다. 최대 곡률은 두 군 간에 유의한 차이가 있었다(대조군: 14.37 ± 5.13, 환자군: 20.67 ± 10.56, p<0.001). 수신자 동작 특성 분석에서 곡선하 면적은 0.711 이었다(95% 신뢰구간; 0.639 - 0.782). 민감도 70.0%, 특이도 62.0% 일 때 양성 우도가 1.84로 최대화하였다. 특이도를 최저 한계값인 50.0%로 설정할 때 민감도 74.8%였고 양성 우도는 1.50 이었다.

결론

제안된 소프트웨어는 조기 망막신경섬유층 결손의 진단에 유용하게 사용될 수 있다.

주요어: 컴퓨터 보조 진단, 안저 촬영, 망막신경섬유층, 녹내장

학번: 2013-21692